



HAL
open science

Modelling the role of HIF in the regulation of metabolic key genes LDH and PDH: Emergence of Warburg Phenotype

Kévin Spinicci, Pierre Jacquet, Gibin Powathil, Angélique Stéphanou

► To cite this version:

Kévin Spinicci, Pierre Jacquet, Gibin Powathil, Angélique Stéphanou. Modelling the role of HIF in the regulation of metabolic key genes LDH and PDH: Emergence of Warburg Phenotype. *Computational and Systems Oncology*, 2022, 2 (3), 10.1002/cso2.1040 . hal-03759747

HAL Id: hal-03759747

<https://hal.science/hal-03759747>

Submitted on 24 Aug 2022

HAL is a multi-disciplinary open access archive for the deposit and dissemination of scientific research documents, whether they are published or not. The documents may come from teaching and research institutions in France or abroad, or from public or private research centers.

L'archive ouverte pluridisciplinaire **HAL**, est destinée au dépôt et à la diffusion de documents scientifiques de niveau recherche, publiés ou non, émanant des établissements d'enseignement et de recherche français ou étrangers, des laboratoires publics ou privés.



Distributed under a Creative Commons Attribution 4.0 International License

1 Modelling the role of HIF in the regulation of metabolic key
2 genes LDH and PDH: Emergence of Warburg Phenotype.

3 Kévin SPINICCI^{1,2}, Pierre JACQUET¹, Gibin POWATHIL², and Angélique
4 STEPHANOU¹

5 ¹Univ. Grenoble Alpes, CNRS, UMR 5525, VetAgro Sup, Grenoble INP, TIMC, 38000
6 Grenoble, France

7 ²Department of Mathematics - Swansea University

8 May 2022

9 **Abstract**

10 Oxygenation of tumours and the effect of hypoxia in cancer cell metabolism is a widely studied
11 subject. Hypoxia Inducible Factor (HIF), the main actor in the cell response to hypoxia, represents
12 a potential target in cancer therapy. HIF is involved in many biological processes such as cell pro-
13 liferation, survival, apoptosis, angiogenesis, iron metabolism and glucose metabolism. This protein
14 regulates the expressions of Lactate Dehydrogenase (LDH) and Pyruvate Dehydrogenase (PDH),
15 both essential for the conversion of pyruvate to be used in aerobic and anaerobic pathways. HIF
16 upregulates LDH, increasing the conversion of pyruvate into lactate which leads to higher secretion of
17 lactic acid by the cell and reduced pH in the microenvironment. HIF indirectly downregulates PDH,
18 decreasing the conversion of pyruvate into Acetyl Coenzyme A which leads to reduced usage of the
19 Tricarboxylic Acid (TCA) cycle in aerobic pathways. Upregulation of HIF may promote the use of
20 anaerobic pathways for energy production even in normal extracellular oxygen conditions. Higher use
21 of glycolysis even in normal oxygen conditions is called the Warburg effect. In this paper, we focus
22 on HIF variations during tumour growth and study, through a mathematical model, its impact on
23 the two metabolic key genes PDH and LDH, to investigate its role in the emergence of the Warburg
24 effect. Mathematical equations describing the enzymes regulation pathways were solved for each
25 cell of the tumour represented in an agent-based model to best capture the spatio-temporal oxygen
26 variations during tumour development caused by cell consumption and reduced diffusion inside the
27 tumour. Simulation results show that reduced HIF degradation in normoxia can induce higher lactic
28 acid production. The emergence of the Warburg effect appears after the first period of hypoxia before
29 oxygen conditions return to a normal level. The results also show that targeting the upregulation of
30 LDH and the downregulation of PDH could be relevant in therapy.

31 Introduction

32 Cells rely on two main processes to produce ATP: Oxidative Phosphorylation (OXPHOS) by using oxygen,
33 and glycolysis by using glucose. Glycolysis is a pathway generating both ATP and pyruvate using glucose
34 as input [1, 2, 3]. Pyruvate produced by glycolysis can then be used to fuel the Tricarboxylic Acid
35 (TCA) cycle and produce the compounds involved in OXPHOS, the aerobic pathway. If oxygen is not
36 present, pyruvate is turned into lactate, this process is called fermentation [4]. Lactate formed during
37 fermentation is secreted into the microenvironment which causes a decrease in extracellular pH.

38 In 1927, Otto Warburg observed that the tumour consumed more glucose and produced more lactic
39 acid than normal tissues [5]. At first Warburg's observation did not consider the presence of oxygen,
40 yet since increased lactic acid production was also observed when oxygen is available, it has slowly been
41 associated with aerobic glycolysis [6]. Nowadays, high rate of glycolysis, even if oxygen is available, is
42 known as the Warburg Effect [7, 8]. In this paper, we will retain this definition. Tumours can develop
43 anywhere, yet harsh conditions favour tumour appearance [9]. Most tumours have median oxygen levels
44 falling below 2%, the threshold at which the hypoxic response is half-maximal [10]. For this reason,
45 a lot of interest has been put in the effect of oxygenation on tumour metabolism and specifically on
46 the Hypoxia Inducible Factor (HIF) protein. This protein, being the main actor in the cell response to
47 hypoxia, is interesting to explore as a potential target for cancer therapy since hypoxic cells are more
48 radioresistant [10, 7].

49 HIF Structure and Mechanism of action

50 The HIF protein was discovered by Semenza and co-workers during a study on the erythropoietin (EPO)
51 gene, a gene encoding for the erythropoietin hormone involved in red blood cells production, in 1991
52 [11]. They found DNA sequences in the gene important for its transcriptional activation in hypoxic
53 conditions, now called Hypoxia Response Elements (HRE). The HIF protein is a heterodimer composed
54 of two subunits HIF-1 α and HIF-1 β , it acts as a transcription factor by binding to HRE in hypoxic
55 conditions. The subunit HIF-1 α is oxygen-sensitive and degraded in presence of oxygen, compared to the
56 constitutively expressed HIF-1 β subunit. Three isoforms of the α subunit have been identified: HIF-1 α ,
57 HIF2- α and HIF3- α . HIF-1 α and HIF2- α are the most studied of the three homologs, HIF-1 α is expressed
58 ubiquitously in the body while HIF2- α expression is tissue-specific [11]. It has been demonstrated that
59 overexpression or suppression of HIF-1 α or HIF2- α influence each other *in vitro* and one homolog can
60 be more expressed than the other. Kidney lesions with early VHL inactivation show more activation of
61 HIF-1 α than HIF-2 α but this balance can change [12]. Transcriptional activity of HIF-1 α requires the
62 binding of the co-factor CBP/p300 to the C-TAD domain of HIF-1 α , then HIF will bind to HRE and
63 activate the transcription of its target genes [11, 13, 14].

64 HIF regulation

65 Oxygen-dependent regulation of HIF-1 α is mainly done by Prolyl Hydroxylase (PHD) and FIH-1 en-
66 zymes. They act at the posttranslational level by inducing its degradation or disrupting its interaction

67 with co-factors. Prolyl Hydroxylase (PHD) proteins catalyze the hydroxylation of proline residues, tar-
68 geting HIF-1 α for proteasomal degradation by the Von Hippel-Lindau (VHL) tumour suppressor protein.
69 Hydroxylation of asparagine residues by Factor Inhibiting HIF-1 (FIH-1) inhibits the interaction between
70 HIF-1 α and the important co-factor CBP/p300, preventing regulation of HIF-1 α target genes. Since
71 PHD and FIH-1 need oxygen to hydroxylate HIF-1 α residues, they act as oxygen sensors in the cell
72 response to hypoxia. Hypoxia promotes HIF-1 α protein stability and transcriptional activity. Reactive
73 Oxygen Species (ROS) and oncometabolites such as succinate, fumarate, lactate upregulate HIF-1 α [14].

74 Oxygen-independent mechanisms regulating HIF-1 α transcription and translation include PI3K/Akt/
75 mTOR and RAS/RAF/MEK/ERK pathways. Multiple growth factors, oncogenes, mutations (such as
76 in the tumour suppressor genes PTEN and p53) or ROS may increase HIF-1 α levels through PI3K and
77 RAS signalling cascade [14, 11, 13]. A study by The Cancer Genome Atlas (TCGA) identified the most
78 altered genes in glioblastoma, it reveals that RTK/RAS/PI3K are among the frequently altered pathways
79 in this disease [15]. It suggests that HIF is a strong candidate for cancer therapy, not only because of
80 its role in the cellular response to hypoxia but also for its frequent deregulation in cancer as well. HIF
81 regulation is summarized in figure 1.

82 **Impact on cellular biological functions**

83 The cell response to hypoxia initiated by HIF affects many biological processes such as cell proliferation,
84 survival, apoptosis, angiogenesis, iron metabolism and glucose metabolism [13]. Pathway enrichment
85 analysis of 98 HIF target genes revealed 20 pathways including those implicated in cancer, glycoly-
86 sis/gluconeogenesis and metabolism of carbohydrates [16].

87 HIF can prevent G1/S transition through the regulation of cyclin-dependent kinase inhibitors (p21,
88 p27) and cyclin proteins (cyclin G2, cyclin E) [17]. Cyclin E downregulation is mediated through the
89 inhibition of cyclin D by HIF causing a slowing down or arrest of the cell cycle in the G1 phase and
90 promoting the entry into quiescence, which can be a mechanism to escape chemotherapy [18].

91 The Tricarboxylic Acid (TCA) cycle (also called Citric Acid or Krebs Cycle) is a circular process fueled
92 by AcetylCoA generating NADH and FADH₂ for its use in the Oxidative Phosphorylation (OXPHOS)
93 pathway. Although OXPHOS is the main pathway generating ATP, TCA produce energy in the form of
94 GTP (equivalent of ATP). These processes represent the aerobic pathways used by the cell when oxygen
95 is present for ATP production. Pyruvate produced by the last steps of the glycolysis is turned into
96 Acetyl Coenzyme A by Pyruvate Dehydrogenase (PDH) to fuel the TCA cycle, promoting an oxidative
97 metabolism [4, 19]. However, Pyruvate Dehydrogenase Kinase (PDK) an inhibitor of PDH is upregulated
98 by HIF [20].

99 When oxygen is not present, the Lactate Dehydrogenase (LDH) enzyme catalyze the reaction in
100 which pyruvate formed by the glycolysis is turned into lactate to generate NAD⁺. This last step allows
101 glycolysis to continue in anaerobic condition since NAD⁺ is required for pyruvate production. In presence
102 of oxygen, NAD⁺ availability is ensured by OXPHOS [4, 19].

103 Different isoforms of both LDH and PDH enzymes exist. Those isoforms present several differences
104 like kinetics parameters, the tissue or the cellular compartment where the isoforms is expressed. For

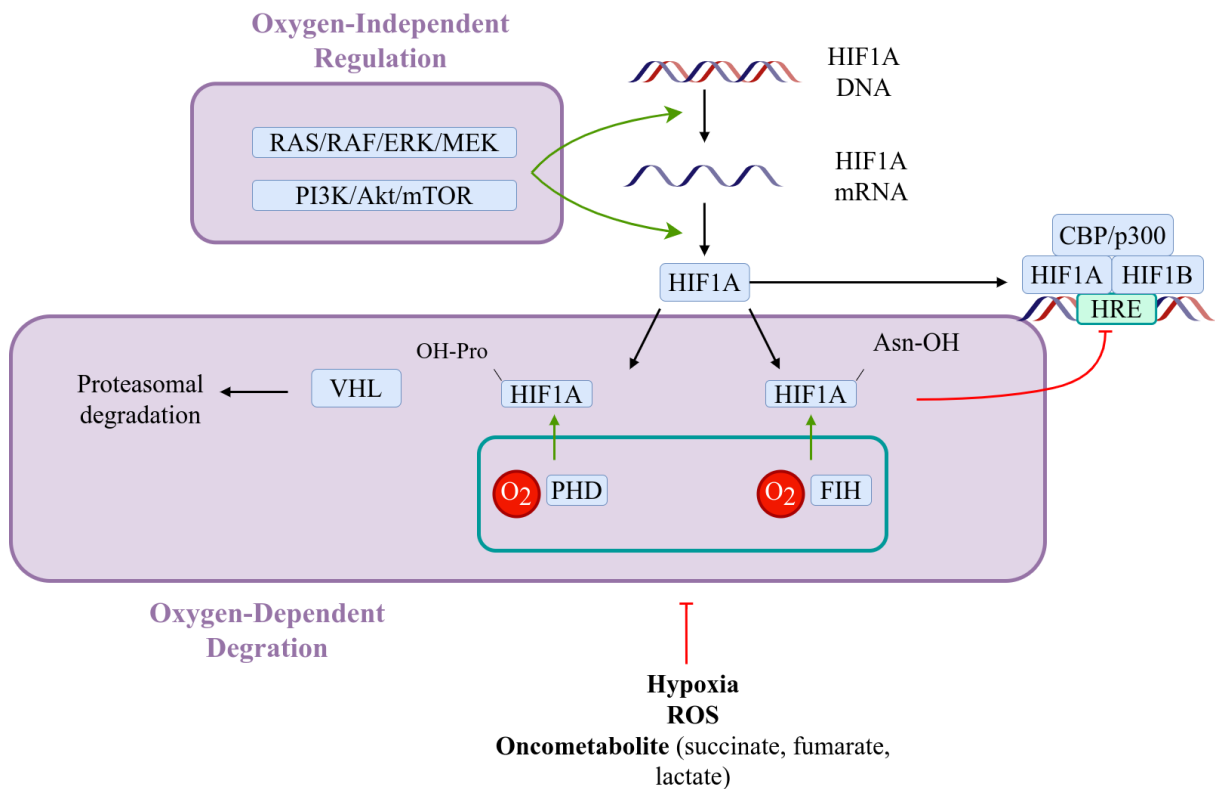


Figure 1: Regulation of Hypoxia Inducible Factor by oxygen-dependent and oxygen-independent mechanisms. PI3K/Akt/mTOR and RAS/RAF/ERK/MEK signalling pathways increase HIF transcription and translation in an oxygen-independent way. The oxygen-dependent regulation relies mainly on the two enzymes: PHD and FIH-1. PHD catalyzes the oxygen-dependent hydroxylation of proline residues on the HIF protein, which is then targeted for proteasomal degradation by the VHL. FIH-1 catalyzes the oxygen-dependent hydroxylation of asparagine residues, which inhibits the interaction between the HIF protein and the CBP/p300 co-factor. Hydroxylation of HIF residues by PHD and FIH-1 is inhibited by hypoxia, ROS and oncometabolites such as succinate, fumarate and lactate.

105 example, LDH-A is expressed in the skeletal muscle LDH-B in heart [21]. LDH-A is also the isoform
 106 comonly upregulated in cancer [22]. The differences between isoforms add a level of complexity. However,
 107 this is out of the scope of this study.

108 The Warburg effect is caused by an increase in glucose utilization by the cells, the glycolysis being
 109 one of the pathways affected by hypoxia. HIF increases the expression of glucose transporters GLUT1
 110 and GLUT3 which contain HRE in their promoters, resulting in higher glucose uptake [23]. Furthermore,
 111 HIF induces the overexpression of specific glycolytic isoforms for each enzyme involved in all the steps
 112 of the glycolysis [21]. Thus, HIF upregulates the expression of LDH, resulting in higher lactate secretion
 113 which acidifies the microenvironment. Not only hypoxia will increase the use of glycolysis by the cell,
 114 but it will also reduce the use of TCA cycle.

115 In this paper, we want to study how genetic (or epigenetic) regulations, between HIF and its two
 116 targets LDH and PDH, may affect the emergence of the Warburg effect. The Warburg effect results in
 117 an increased production of lactic acid by the tumour by metabolizing glucose, even in normoxia [24, 7,
 118 8, 25, 26].

119 Material and Method

120 Genetic Regulations

121 Here, we assume that HIF plays a major role in mediating the cell response to hypoxia. We have
 122 selected LDH and PDH to model the effect of hypoxia on metabolism since (1) they are key enzymes
 123 for the conversion of pyruvate into lactate/AcetylCoA respectively after the glycolysis, and (2) they are
 124 both regulated by HIF directly or indirectly. PDH is downregulated by HIF through its inhibitor PDK,
 125 therefore PDK will be included in the model (see figure 2). Genetic regulations are based on the model
 126 described by Li *et al* [20]. All genetic regulations are described by the following equations:

$$\frac{du}{dt} = A_u - D_u \times H_{O_2 \rightarrow u} \times u \quad (1)$$

$$\frac{dv}{dt} = A_v \times H_{u \rightarrow v} - D_v \times v \quad (2)$$

$$\frac{dw}{dt} = A_w \times H_{u \rightarrow w} - D_w \times w \quad (3)$$

$$\frac{dz}{dt} = A_z \times H_{w \rightarrow z} - D_z \times z \quad (4)$$

127 where u , v , w and z are HIF, LDH, PDK and PDH levels, respectively; A is a parameter for gene
 128 production and D for gene degradation. LDH and PDK upregulations by HIF and PDH downregulations
 129 by PDK are described with a non-linear function named the shifted-Hill function. In the same way, the
 130 increased HIF protein degradation in normoxia is described using the same function. The shifted-Hill
 131 function has the form:

$$H_{Y \rightarrow Z} = \frac{S^n}{S^n + Y^n} + \gamma_{Y \rightarrow Z} \frac{Y^n}{S^n + Y^n}. \quad (5)$$

132 Here, n is the Hill coefficient. S is the gene level with a half-threshold of production. The positive
 133 parameter γ represents an activation if > 1 or an inhibition if < 1 . $H_{Y \rightarrow Z}$ represents the effect of the

Parameter	Value	Dimension	Parameter	Value	Dimension
A_u	0.05	1/min	D_u	0.005	1/min
A_v	0.005	1/min	D_v	0.005	1/min
A_w	0.005	1/min	D_w	0.005	1/min
A_z	0.005	1/min	D_z	0.005	1/min
$S_{O_2 \rightarrow u}$	0.02085	mmol/L	$S_{u \rightarrow v}$	4.48	-
$S_{u \rightarrow w}$	5.0	-	$S_{w \rightarrow z}$	2.2	-
$\gamma_{O_2 \rightarrow u}$	10.0	-	$\gamma_{u \rightarrow v}$	3.61	-
$\gamma_{u \rightarrow w}$	6.97	-	$\gamma_{w \rightarrow z}$	0.14	-

Table 1: Parameters used in genetics regulations. The symbol "-" stands for dimensionless.

134 regulating gene Y on the regulated gene Z , it can be an upregulation if γ is > 1 , or a downregulation if
135 γ is < 1 . All genes levels are dimensionless, parameters used in the equation above are summarised in
136 table 1.

137 Cell Metabolism

Nutrient consumption rates change over time depending on microenvironment conditions. In normoxia, glycolysis transforms glucose to pyruvate, then pyruvate is converted to AcetylCoA by PDH enzymes to feed the TCA cycle. The TCA cycle works in cooperation with OXPHOS to produce ATP using oxygen, which constitutes the aerobic pathway [19]. Since the conversion of pyruvate to AcetylCoA is catalyzed by the PDH enzyme, its availability bounds the use of TCA and should be reflected in the consumption of oxygen. In hypoxia, glucose consumption is increased to produce the ATP needed using aerobic pathways. Pyruvate formed by glycolysis is then turned into lactate by LDH enzymes, increasing acidity in the microenvironment [19]. Like PDH, increased LDH levels should reflect an increased usage of anaerobic pathways with higher consumption of glucose. As PDH and LDH play an important role in the fate of pyruvate, their respective levels should impact cells metabolism in our model.

In equations 6 and 7, we define p_O and p_G , two terms to describe the impact of LDH and PDH on glucose and oxygen consumptions using a sigmoid function based on the logistic function. p_O and p_G will adjust the consumptions rates of oxygen and glucose defined in equations 8 and 9, by increasing or decreasing the maximal rates according to the level of PDH and LDH.

$$p_O = \frac{\phi_O - \psi_O}{1 + \exp(-l_z(z - z_0))} + \psi_O \quad (6)$$

$$p_G = \frac{\phi_G - \psi_G}{1 + \exp(-l_v(v - v_0))} + \psi_G \quad (7)$$

138 Here, ϕ_O and ϕ_G are the maximal values for p_O and p_G . ψ_O and ψ_G are the minimal values for p_O and
139 p_G . z and v are the current level of PDH and LDH. z_0 and v_0 represent the midpoint of p_O and p_G . l_z
140 and l_v represent the steepness of the curve for p_O and p_G .

141 Cells consumption and production are described following the functions from the model defined by [27]
142 (a brief description of the complete model is available in supplementary material).

143 Oxygen consumption is determined using a Michaelis-Menten function [27]:

$$f_O = p_O V_O \frac{O_e}{O_e + K_O} \quad (8)$$

144 PDH allows the pyruvate to enter the TCA cycle as Acetyl Coenzyme A, it is a limiting step in the aerobic
 145 pathway. This is included in the model by adjusting the maximum oxygen consumption rate V_O using the
 146 term p_O to represent PDH level effect on metabolism. O_e is the extracellular oxygen concentration. K_O
 147 is the extracellular oxygen concentration at which the cell oxygen consumption rate is half-maximum.

148 Following Robertson-Tessi *et al* [27], we assume that ATP demand drives glucose consumption. In low
 149 oxygen conditions, the cell will consume more glucose to produce ATP in the last step of the glycolysis,
 150 then pyruvate is turned into lactate by the LDH enzyme. An increase of LDH indicates an upregulation
 151 of anaerobic pathways which means here, an increase in glucose consumption. We use the term p_G to
 152 increase glucose consumption in the equation 9 when levels of LDH increase [27].

$$f_G = \left(\frac{p_G A_0}{2} - \frac{29 f_O}{10} \right) \frac{G_e}{G_e + K_G} \quad (9)$$

153 A_0 is the target ATP production. G_e is the extracellular glucose concentration. K_G is the extracellular
 154 glucose concentration at which the glucose consumption rate is half-maximal.

155 In this paper, we are studying how HIF can impact the interplay between aerobic (TCA + OXPHOS) and
 156 anaerobic (glycolysis + lactate secretion) pathways to generate ATP, due to its PDH and LDH enzymes
 157 important for conversion of pyruvate. Therefore, we do not directly model aerobic and anaerobic pathways
 158 but rather we compute the theoretical level of ATP generated by both processes (equation 12). We take
 159 the same stoichiometric coefficients as in [27]: glycolysis uses 1 mole of glucose produces 2 moles of ATP,
 160 aerobic pathway uses 1 mole of glucose and 5 moles of oxygen to produce 29 moles of ATP. We can
 161 compute the ATP produced from the nutrients consumed using the yield from glycolysis and aerobic
 162 pathway [27]:

$$f_A = 2f_G + \frac{29f_O}{5} \quad (10)$$

163 Glycolysis produces 2 moles of pyruvate with 1 mole of glucose. If oxygen is absent, pyruvate is turned
 164 into lactate, giving a total of 2 moles of lactate [4]. Lactic acid production is given by the glucose
 165 consumed:

$$f_{H^+} = k_H 2f_G \quad (11)$$

k_H is a fixed parameter for proton buffering (dimensionless).

Quantity of ATP produced by the cell is modelled by an ODE, and extracellular quantities of the three
 molecules oxygen (O), glucose (G) and protons (H^+) are described by PDEs in the following equations:

$$\frac{dA}{dt} = f_A \quad (12)$$

$$\frac{\partial O}{\partial t} = D_O \nabla^2 O - \sum_{k=1}^{N_i} f_O^k \quad (13)$$

$$\frac{\partial G}{\partial t} = D_G \nabla^2 G - \sum_{k=1}^{N_i} f_G^k \quad (14)$$

$$\frac{\partial H^+}{\partial t} = D_{H^+} \nabla^2 H^+ + \sum_{k=1}^{N_i} f_{H^+}^k \quad (15)$$

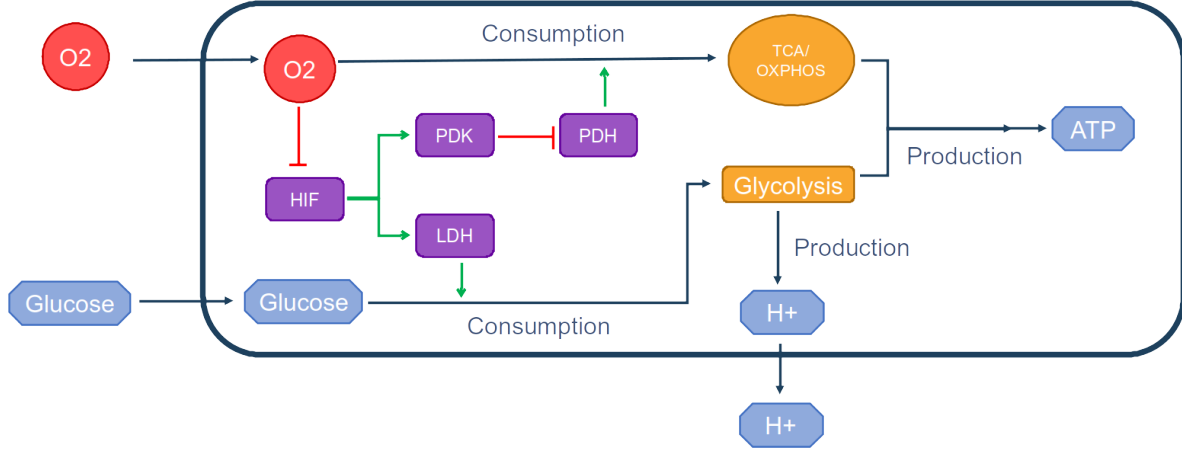


Figure 2: Cell metabolism and genetic regulations implemented in the model. Green arrows represent upregulation, red arrows represent inhibition.

166 D_O , D_G and D_{H^+} are the diffusion coefficient for each molecules. N_i is the number of cells in the
 167 voxel i . Initial values for oxygen in equation 13 are $O(x, y, 0) = 0.056$ mmol/L in normoxia and 0.012
 168 mmol/L in hypoxia. Initial value for glucose in equation 14 is $G(x, y, 0) = 5.0$ mmol/L. Initial value for
 169 protons in equation 15 is $H^+(x, y, 0) = 3.98 \cdot 10^{-5}$ mmol/L (pH 7.4). Let x_0 and y_0 the lower boundary
 170 of the domain in x and y , x_L and y_L the upper boundary in x and y . Boundary values for oxygen in
 171 equation 13 are $O(x_0, y, t) = O(x_L, y, t) = O(x, y_0, t) = O(x, y_L, t) = 0.056$ mmol/L in normoxia and
 172 0.012 mmol/L in hypoxia. Boundary values for glucose in equation 14 are $G(x_0, y, t) = G(x_L, y, t) =$
 173 $G(x, y_0, t) = G(x, y_L, t) = 5.0$ mmol/L. Boundary values for H^+ in equation 15 are $H^+(x_0, y, t) =$
 174 $H^+(x_L, y, t) = H^+(x, y_0, t) = H^+(x, y_L, t) = 3.98 \cdot 10^{-5}$ mmol/L (pH 7.4). Parameters used in those
 175 functions are summarised in Table 2. The schematic in figure 2 shows the cellular metabolism and the
 176 genetics regulation implemented in the model.

177 Numerical Implementation

178 The tumour microenvironment plays a vital role in the growth and progression of tumour cells. As the
 179 tumour grows, intracellular and intercellular interactions influence the changes in its microenvironment,
 180 which can further result in cells dynamic. Here, we aim to develop a modelling framework to simulate the
 181 growth of a large population of cells cultured *in vitro*, each cell having its metabolism influenced by the
 182 microenvironment conditions to represent accurately the resources dynamics in the tumour. Therefore,
 183 the numerical implementation of the model must have sufficient performance to simulate the behaviour
 184 of thousands of cells. In this regard, we selected Physicell, an open-source C++ framework designed
 185 to run simulations containing a large population of cells. This framework has good performance with a
 186 low memory footprint, allows the user to implement his custom code and define custom cell types, run a
 187 multi-agent-based simulation in 2D or 3D [28].

188 Most aspect of the model are handled by the physicell software [28], this includes : cell division and
 189 progression through the cell cycle, cell adhesion and repulsion, substrate diffusion, cell exchanges with

Parameter	Value	Unit
V_O	0.01875	mmol/L/min
K_O	0.0075	mmol/L
K_G	0.04	mmol/L
k_H	2.5e-4	-
A_0	0.10875	mmol/L/min
ϕ_G	50	-
ψ_G	1	-
l_G	4	-
v_0	2.35	-
ϕ_O	1	-
ψ_O	0	-
l_O	15	-
z_0	0.575	-
D_O	109,200	$\mu\text{m}^2/\text{min}$
D_G	30,000	$\mu\text{m}^2/\text{min}$
D_{H^+}	27,0000	$\mu\text{m}^2/\text{min}$

Table 2: Parameters for metabolism. The symbol "-" stands for dimensionless.

190 the environment (secretion and consumption). Cells are modelled with the shape of a sphere that cannot
191 deform, adhesion and repulsion are implemented using a potential function. The cell division process is
192 implemented as a cycle, where the user can define each steps and and progression between them. There
193 is no condition on the neighbourhood, a cell will divide even if it is surrounded by other cells as long
194 as there is sufficient nutrient. As a consequence, certain regions of the tumour will exhibit a higher cell
195 density. We implemented in Physicell an heterogeneous diffusion with respect to local cellular density.
196 In the model, phases duration are 5h in G1, 8h in S, 4h in G2 and 1h in M, for a total of 18h to complete
197 a cell cycle [29].

198 Here, the impact of extracellular oxygen concentration is studied considering different boundary con-
199 ditions: physiological normoxia at 0.056 mmol/L (5% O_2), pathological hypoxia at 0.01112 mmol/L (1%
200 O_2) and a last where boundary conditions are modified during the simulation from physiological normoxia
201 to pathological hypoxia. The hypoxia threshold is set at 0.02085 (2% O_2), the level at which HIF has a
202 half-maximal response [10].

203 The governing ODEs (equation 1 - 4 and 12) and PDEs (equation 13 - 15) are run at each timestep to
204 compute cell nutrient consumption, energy and acidity production for that period. After each time step,
205 the cell state is updated according to the quantity of ATP generated and the extracellular pH. Therefore,
206 cells can proliferate and divide only if they were able to generate enough ATP and if extracellular pH
207 is higher than the acid resistance of the cell (6.1 [27]). If the quantity of ATP generated is less than a
208 threshold $ATP_{\text{quiescence}}$, the cell enters quiescence and is then prevented to complete the G1 phase. If the

209 quantity of ATP generated is less than a threshold ATP_{death} or if the pH is less than a threshold pH_{death} ,
210 the cell dies and enters into the death cycle where it is progressively removed from the microenvironment
211 by lysis.

212 To simulate the cell entry into quiescence, we created a phase G0 with a reversible link to the G1
213 phase of the cell cycle. If the condition for proliferation are not met, we set the transition rate from G1
214 to G0 at a maximum value and the rate from G0 to G1 at 0. The cell is forced to enter the G0 phase
215 and is prevented to transit to the G1 phase to continue its division. Once the level of ATP rises again,
216 we revert the transition rates values to allow the cell to leave the G0 phase and divide anew. The cell
217 can only transit to the G0 phase from the G1 phase, thus it will complete its cycle once it leaved the G1
218 phase and will divide even if ATP levels fall while the division process is ongoing.

219 Results

220 Qualitative exploration of the model at the cell scale

221 A well-known phenomenon is the Warburg effect, increased production of lactic acid by the tumour [5]
222 even in normoxia [24, 7, 8]. A qualitative study of the genetic deregulations at the cell scale would reveal
223 how it impacts lactic-acid production to investigate the appearance of the Warburg effect. The primary
224 aim of this study is to investigate the role of genetic regulations in cell metabolic changes.

225 In our mathematical model, the regulating effect of a gene on another is mainly driven by the γ
226 parameter in the shifted-Hill function. Setting this parameter equal to 1 simulate a loss of the regulating
227 function. An over-sensitivity of a gene by its regulator is modelled by setting the γ parameter to 40, the
228 maximum defined in the model from [20]. Results of a few regulations are shown in figure 3.

229 When no genetic deregulations are applied to the model (figure 3.A), protons production range from
230 0.0001 mmol/L/min to 0.001 mmol/L/min with normal γ parameters. Around 0.01 mmol/L oxygen
231 (1%), the cell progressively increases its H^+ secretion rate from 0.0001 mmol/L/min to the maximum
232 0.001 mmol/L/min.

233 In our model, when HIF is not subjected to oxygen degradation (figure 3.B), the rate of H^+ production
234 is only influenced by glucose concentration. In this case, cell's lactic-acid secretion rate can reach 0.001
235 mmol/L/min even in normal oxygen pressure, as a result of the Warburg effect. Increased degradation of
236 HIF in oxygen (figure 3.C) reduces the oxygen threshold at which the cell has a lactic-acid secretion rate
237 of 0.001 mmol/L/min. Lower levels of oxygen are needed to reach the maximal secretion rate compared
238 to the normal degradation rate of HIF. With no deregulation (figure 3.A), the lactic-acid secretion rate
239 starts to increase at around 0.019 mmol/L of oxygen and reach a maximum at around 0.08 mmol/L.
240 With increased HIF degradation by oxygen (figure 3.C), this span is reduced and lactic-acid secretion
241 increases at around 0.012 mmol/L of oxygen. Similar to our result, a model from [25] shows that a lower
242 degradation rate of HIF increases the chance that cells use glycolysis instead of OXPHOS, which will
243 increase lactic acid secretions.

244 Inhibiting LDH sensitivity to HIF (figure 3.D) causes the maximum lactic-acid secretion rate to fall
245 to 0.0008 mmol/L/min. Increasing LDH sensitivity to HIF does not permit the cell to have a higher

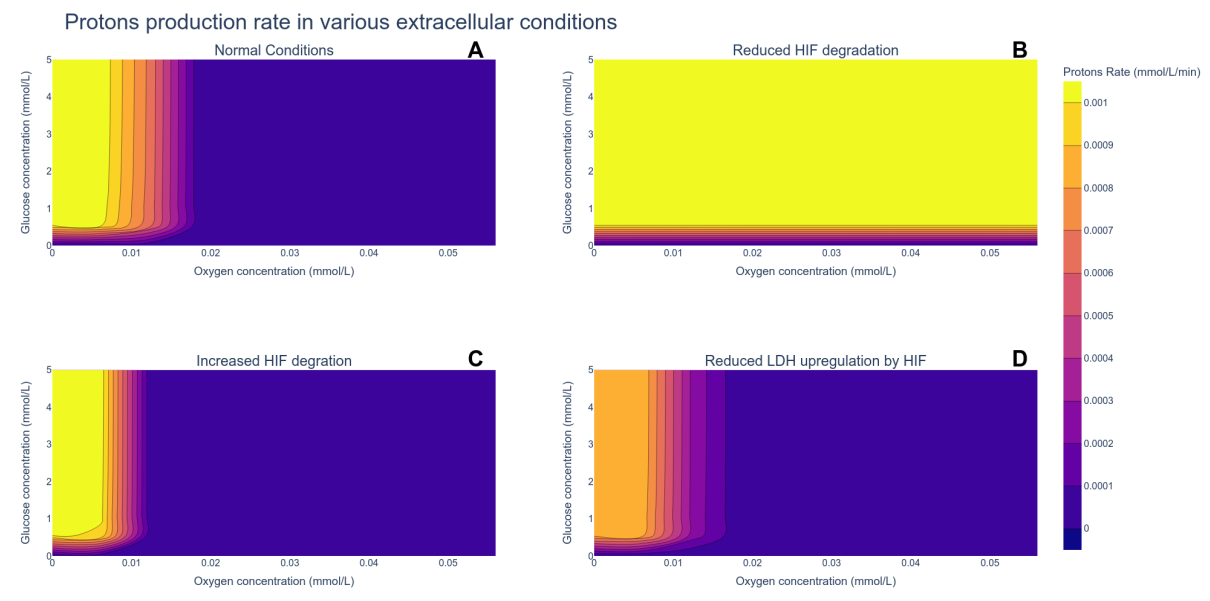


Figure 3: Influence of genetic upregulation or inhibition on the production rate of protons at different glucose and oxygen concentrations. (A) Result with no genetic deregulation. ($\gamma_{O_2 \rightarrow u} = 10.0$, $\gamma_{u \rightarrow v} = 3.61$, $\gamma_{u \rightarrow w} = 6.97$, $\gamma_{w \rightarrow z} = 0.14$) (B) Result with inhibition of the oxygen-dependant degradation of HIF. ($\gamma_{O_2 \rightarrow u} = 1.0$, $\gamma_{u \rightarrow v} = 3.61$, $\gamma_{u \rightarrow w} = 6.97$, $\gamma_{w \rightarrow z} = 0.14$) (C) Result with over-degradation of HIF by oxygen. ($\gamma_{O_2 \rightarrow u} = 40.0$, $\gamma_{u \rightarrow v} = 3.61$, $\gamma_{u \rightarrow w} = 6.97$, $\gamma_{w \rightarrow z} = 0.14$) (D) Result with loss of upregulation of LDH by HIF. ($\gamma_{O_2 \rightarrow u} = 10.0$, $\gamma_{u \rightarrow v} = 3.0$, $\gamma_{u \rightarrow w} = 6.97$, $\gamma_{w \rightarrow z} = 0.14$)

246 H^+ production rate in normoxia, while a decrease prevents a high H^+ production rate in hypoxia (results
247 not shown).

248 Interfering with PDK sensitivity to HIF or PDH sensitivity to PDK seems to have no effect on acid
249 production in the model but on oxygen consumption by the cell (results not shown).

250 Exploration of environment and genetic properties on the emergence of the Warburg phe- 251 notype

252 *Influence of environmental oxygen conditions*

253 The Warburg effect is currently defined as high production of acidity due to the use of glycolysis even in
254 normoxia [25, 26, 9]. We ran several simulations with different environmental oxygen conditions to assess
255 whether microenvironmental conditions only, can induce a Warburg effect in the model.

256 Figure 4 shows how oxygen conditions affect tumour growth. In oscillating conditions, the oxygen
257 concentration varies between physiological normoxia and pathological hypoxia and reverse every 6 hours
258 until the end of the simulation. Kinetics of HIF show a peak after 6h and a decrease to an equilibrium
259 state after 24h-48h. We choose to simulate 6h-period of hypoxia/normoxia to avoid the cell reaching an
260 equilibrium and to simulate stressful conditions with a high response to a low level of oxygen. Constant
261 hypoxia slows down tumour growth and reduces tumour diameter compared to normoxia. In all 3 dif-
262 ferent conditions, the centre of the tumour is composed of dead cells surrounded by living cells at the

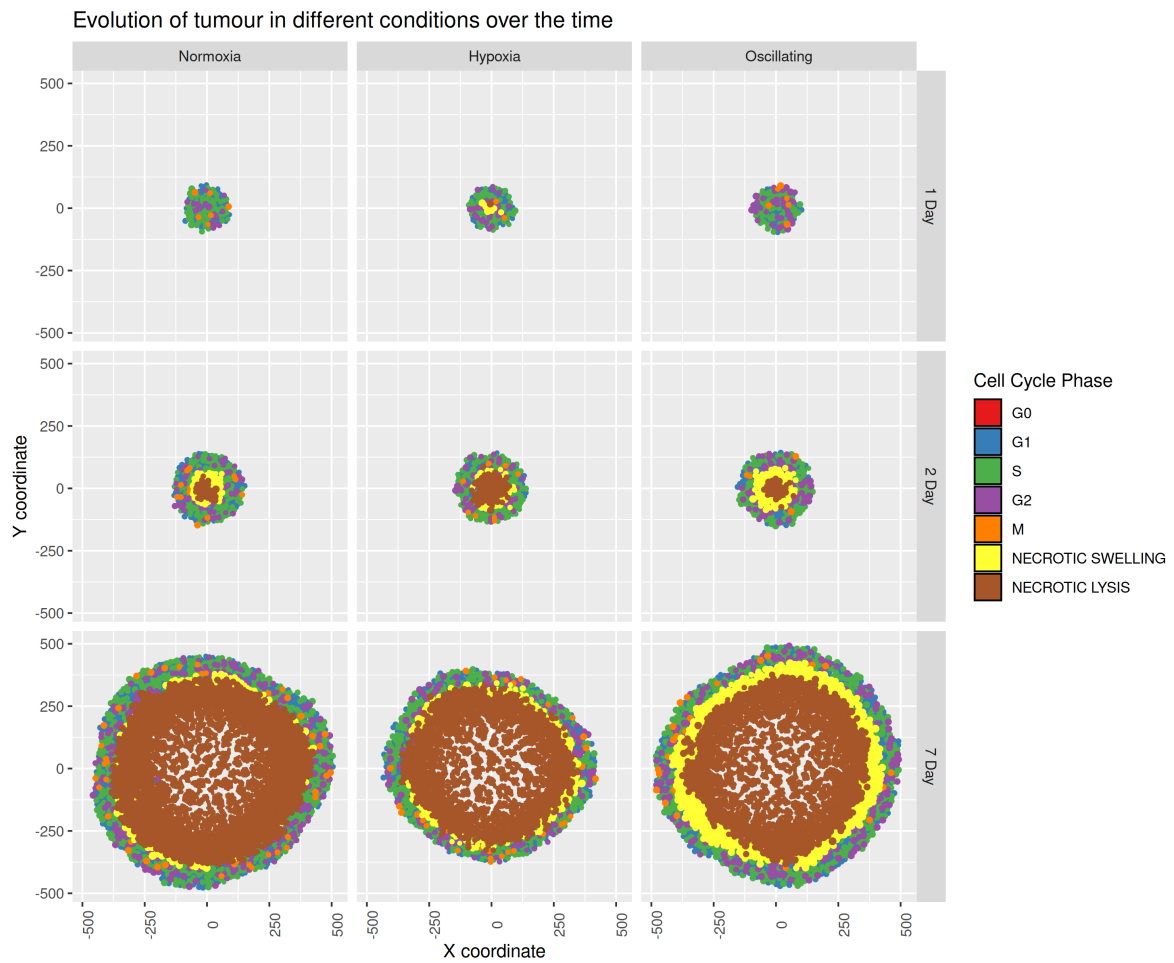


Figure 4: Evolution of tumour growth at different times in different conditions. In oscillating conditions, the oxygen concentration is slowly decreased from normoxia to hypoxia during 6 hours, then cells are slowly put back in normoxia at the same rate. This process is repeated until the end of the simulation.

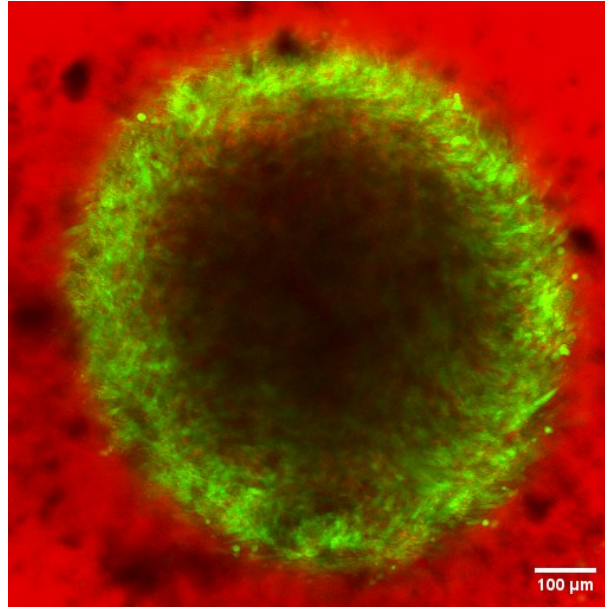


Figure 5: Picture of a spheroid grown for 30 days in an experiment run in the laboratory. Cells were marked using the fluorescent proteins Green FLuorescent Protein (GFP) and Sulforhodamine B (SRB). Living cells are colored in green, dying cells appear in red. The centre of the tumour is composed of hypoxic and dead cells, both do not emit fluorescence.

263 periphery. Only in normoxia and varying oxygen conditions, some cells in the centre of the tumour do
264 continue to divide (only visible after 7 days of growth). This may be due to the changes in the tumour
265 microenvironment with the increased cell death at the centre. As the cells die, more nutrients will be
266 available to quiescent cells to enable them to reenter proliferating phase. Moreover, spatial changes due
267 to the shrinkage of dead cells can influence the availability of nutrients at the centre. This might show a
268 mechanism by which the tumour can grow back after a period of harsh conditions, for example quiescence
269 can be a mechanism to avoid drugs effect for the tumour cell [30]. Necrotic core has been observed in
270 biological experiments run in the lab (figure 5).

271 It seems that varying the concentration of oxygen from normoxia to hypoxia, and reversing this
272 process, every 6 hours does not affect the diameter of the tumour at the end of the simulation. However,
273 a ring of necrotic cells in the swelling phase appears thicker than in other conditions.

274 Results in figure 6 show acid production according to the extracellular oxygen concentration. Red
275 line y-axis intercept is equal to 0.02085 mmol/L (2% O₂), which corresponds to the threshold of hypoxia
276 in physiological conditions. It is the level at which HIF has a half-maximal response as well [10]. Cells
277 above this level are considered to be in normoxia while the rest of the cells are in hypoxia. Levels of
278 extracellular oxygen fall below the hypoxia threshold after 2 days of growth in normoxic conditions (a
279 necrotic core in the centre of the tumour has already formed). Due to poor oxygen concentration, cells
280 with higher glycolytic activity appear and reach a H⁺ production rate of almost 5×10^{-4} mmol/L/min.
281 The maximum glycolytic activity of cells falls at 7 days of growth because of reduced glucose availability.
282 When tumour growth is started in hypoxic conditions, high glycolytic activity is present after only one
283 day of growth. In those conditions, the way the cell produces its energy is influenced only by glucose

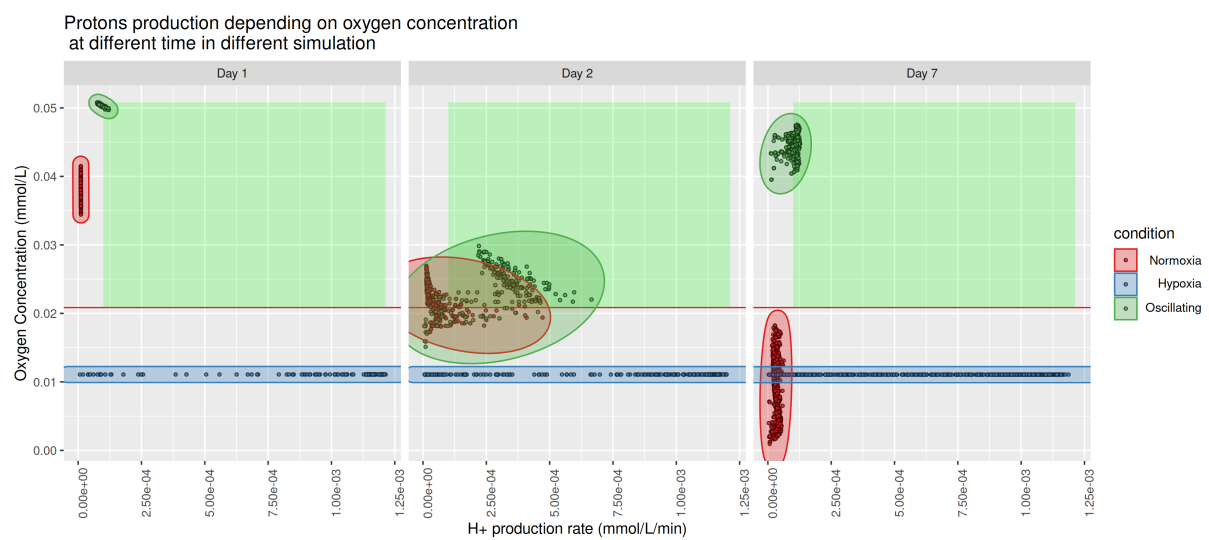


Figure 6: Acid production rate following oxygen extracellular concentrations at different times in different conditions. The red line indicates the hypoxia threshold. In oscillating conditions, oxygen concentration is slowly decreased from normoxia to hypoxia during 6h, then oxygen is increased to normoxia at the same rate. This process is repeated until the end of the simulation. Only living cells are represented on the graph. The green rectangle represents the region corresponding to a Warburg effect.

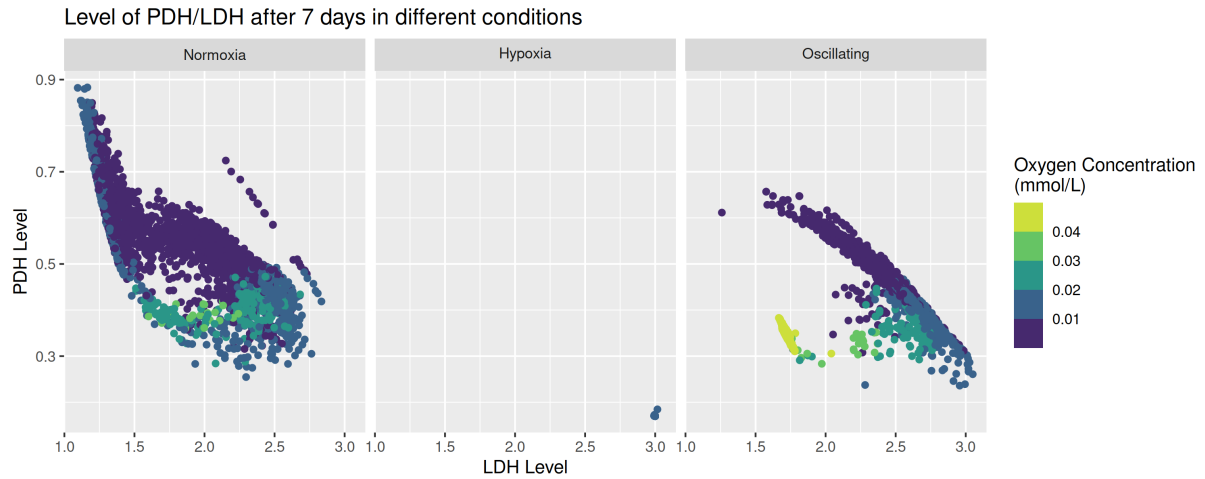


Figure 7: Plot of level of PDH against the level of LDH coloured by the extracellular oxygen concentration. The graph shows the results after 7 days of growth for different conditions. In oscillating conditions, oxygen concentration is slowly decreased from normoxia to hypoxia during 6h, then oxygen is increased to normoxia at the same rate. This process is repeated until the end of the simulation. Only living cell are represented on the graph.

284 concentrations (similar to the result shown in figure 3). Therefore, hypoxic conditions directly select cells
 285 with high glycolytic activity.

286 The fact that, in the model, hypoxia may select cells with high glycolytic activity is supported by the
 287 levels of LDH/PDH genes presented in figure 7. In normoxia, cells have a level of LDH and PDH of 1 for
 288 both, it can be associated to an oxidative state. In hypoxia, LDH level reaches 3.0 and PDH level falls to
 289 0.25, it can be associated to a glycolytic state. At the beginning of the simulation in normoxic conditions,
 290 cells have 1:1 LDH/PDH levels. As the simulation goes, oxygen becomes less available. Thus LDH level
 291 increases while PDH level decreases. The result in normoxic conditions shows that cells migrate from an
 292 oxidative to a glycolytic state as oxygen concentration decreases. Cells around 2:0.5 LDH/PDH levels
 293 have a hybrid state where they rely on both nutrients to produce ATP. Again hypoxia selects for cells
 294 with high levels of LDH and low levels of PDH, suppressing the possibility for the cell to adopt a hybrid
 295 state.

296 Interestingly, extracellular oxygen concentration after 7 days is higher when oxygen varies between
 297 normoxia and hypoxia every 6 hours than in constant normoxia. Since cells are put in hypoxia several
 298 times a day, they rely more on glycolysis and consume less oxygen. Cells with higher glycolytic activity
 299 (2.5×10^{-4} mmol/L/min) even above the threshold of hypoxia appear at 2 days. It suggests that the
 300 Warburg Effect can be caused by environmental conditions with rapid variations. Combined with figure
 301 7, genetic levels seems to indicate that cells cannot enter a complete oxidative state and are trapped
 302 either in a hybrid or a glycolytic state.

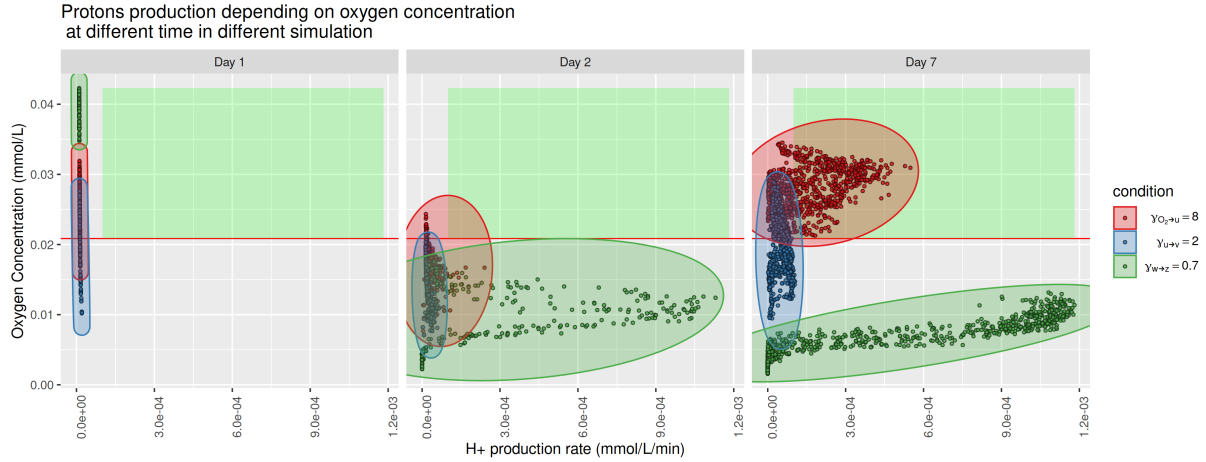


Figure 8: Acid production rate following oxygen extracellular concentrations at different times with different genetic perturbations. The red line indicates the hypoxia threshold. Only living cell are represented on the graph. Three genetics perturbations have been selected: reduced oxygen induced degradation of HIF ($\gamma_{O_2 \rightarrow HIF} = 8.0$), lower use of glycolysis in hypoxic conditions ($\gamma_{HIF \rightarrow LDH} = 2.0$) and lower effect of hypoxia on oxygen consumption ($\gamma_{PDK \rightarrow PDH} = 0.7$). Tumour growth was initiated in normoxia. The green rectangle represents the region corresponding to a Warburg effect.

303 *Influence of the intrinsic genetic properties of the cell*

304 Here, tumour growth is initiated in normoxia (results not shown). Extracellular oxygen concentrations
 305 only vary due to cells consumption and reduced diffusion in the tumour. Only genetics regulations have
 306 been modified between each simulation to assess the impact of different genetic deregulations (muta-
 307 tions or epigenetic alterations) on tumour growth and cell metabolism. Results are similar to normoxic
 308 conditions with no genetic deregulations (presented in figure 4). When reducing inhibition of PDH by
 309 PDK, tumour radius at 7 days of growth is lower than in normoxia and higher than in hypoxia with no
 310 mutation.

311 Figure 8 shows that cells start to become hypoxic after day 1, reaching a majority by day 2. After 7
 312 days with a reduced HIF degradation rate by oxygen, extracellular oxygen goes back to normoxic levels
 313 yet cells have a higher acid production rate that corresponds to a Warburg effect. In this case, we suppose
 314 that cells slowly drain oxygen levels in the environment to a point where hypoxia is reached. Due to
 315 poor oxygen conditions, cells adapt their metabolism to enter a glycolytic state that they keep even if the
 316 oxygen supply goes back above 2 %O₂. Together with the result in figure 9, this might be caused by a
 317 delay in the response from returning to normal conditions since HIF regulation by O₂ is affected. While
 318 some cells have levels of LDH greater than 2 and PDH lower than 0.50 (hybrid to glycolytic state), some

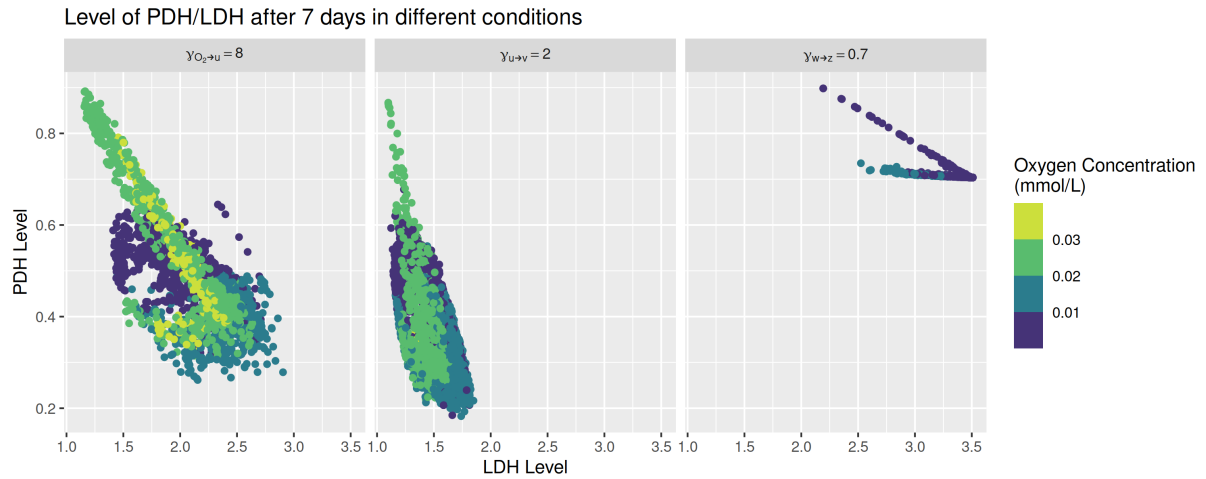


Figure 9: Plot of level of PDH against the level of LDH coloured by the extracellular oxygen concentration. The graph shows the results after 7 days of growth with three different genetic perturbations: reduced oxygen induced degradation of HIF ($\gamma_{O_2 \rightarrow HIF} = 8.0$), lower use of glycolysis in hypoxic conditions ($\gamma_{HIF \rightarrow LDH} = 2.0$) and lower effect of hypoxia on oxygen consumption ($\gamma_{PDK \rightarrow PDH} = 0.7$). Tumour growth was initiated in normoxia.

319 have a ratio of LDH/PDH almost equal to 1:1. This suggests that the Warburg Effect is not irreversible
 320 with a reduced HIF degradation rate by oxygen alone.

321 As expected, reducing the increase in LDH levels due to HIF response does not induce a high acid-
 322 ification rate in normoxia but affects the maximum acid production rate and level of LDH. Instead of
 323 inducing a glycolytic phenotype, it seems to repress it.

324 Reducing the inhibiting power of PDK on PDH allows the cell to keep a higher PDH level, a key
 325 enzyme for oxygen consumption and oxidative state in the model. Cells exhibit an acid production rate
 326 similar to those in hypoxic conditions after 2 and 7 days, compared to other genetics deregulation. While
 327 in normoxia with no genetic deregulation cells seem to fluctuate around the threshold of hypoxia, here
 328 they are all below this level. Since PDH is not effectively regulated by HIF, the cell tends to stay in an
 329 oxidative state and rely less on glycolysis. We can suppose that cells consume oxygen even when the level
 330 fall, creating further harder conditions. Results also show that adaptation to hypoxia is delayed and the
 331 cell only adopts a glycolytic state at oxygen conditions near-pathological hypoxia. PDH levels do not fall
 332 far below 0.75 even after 7 days of growth compared to others conditions, indicating that cells can only
 333 adopt an oxidative or hybrid state.

334 Discussion

335 In this paper, we formulated a mathematical model to study the impact of HIF on LDH and PDH,
 336 key enzymes of glycolysis and TCA cycle and thus investigating its role in cellular metabolism. Since
 337 its discovery, HIF has been actively studied by the scientific community. There are several modelling
 338 approaches to study the effects of HIF [27, 20, 18, 25] and here, we investigate its role using a multi-agent

339 model, considering a heterogeneous environment that changes over time. Furthermore, the model is used
340 to investigate the impact of genes on metabolism and the effect of different environmental conditions and
341 different genetic deregulations (such as mutations or epigenetic alterations) can have on the Warburg
342 Effect, an overproduction of acidity due to and increased glycolysis even in normoxia. Over-production
343 of lactate can also be caused by reduced use of pyruvate in the mitochondria, remaining pyruvate is then
344 turned into lactate.

345 Using the level of LDH and PDH genes as markers, we can define three different metabolic states like
346 [20, 25]: oxidative, glycolytic and hybrid. The oxidative state corresponds to a high level of PDH and
347 a low level of LDH, and inversely in a glycolytic state. The hybrid state then corresponds to medium
348 levels of both enzymes, 2:0.5 for LDH and PDH respectively. As expected, normoxia strongly selects for
349 the first state while hypoxia selects for the second one. The hybrid state is observed as the oxygen levels
350 change over time due to tumour growth. Thus it appears that the cell adopts this state when adapting
351 to changing oxygen conditions or when oxygen levels vary between normoxia and hypoxia several times
352 during tumour growth (oscillating conditions in the model).

353 We observed some differences between our model and the model in a recent paper from Li *et al* [20]: (1)
354 they identified a normal state with a level of LDH at 1 and a level of PDH at 0.1, (2) their oxidative
355 and glycolytic states have different levels of genes than those present in our model. This difference in the
356 result can be explained by the fact that we only include a small fraction of their gene regulation network
357 in our model, to only account for the effect caused by HIF.

358 We have simulated tumour growth when oxygen supply does not vary over time, hence differences in
359 extracellular oxygen level can only be caused by cell consumption or reduced diffusion owing to higher
360 cell density. We found that when there are rapid changes in oxygen supply to the tumour, cells with
361 higher glycolytic rates above the threshold of hypoxia appear. It shows that varying microenvironmental
362 conditions are sufficient to induce a Warburg phenotype for the cell. The results are inline with the
363 findings by Damaghi *et al* [9]. However, the model does not include sudden genetic mutation which
364 can be caused by harsh conditions. Therefore, in our case cell would not be trapped into a Warburg
365 phenotype and this state can be reversed to a normal state if the cell is given enough time in favourable
366 conditions. Lactate secretion, which decreases the extracellular pH, depends on glucose consumption. A
367 study from Casciari *et al* [31] has shown that a lower extracellular pH decreases dramatically glucose
368 consumption, the Warburg effect could also be inhibited by low pH (6.95). We may suppose that after
369 difficult conditions genes may be over-expressed or inhibited which will force the cell to adopt a Warburg
370 phenotype.

371 The importance of HIF degradation in normoxia is further highlighted by the model results. We
372 were also able to induce a Warburg effect by reducing the degradation rate of HIF by oxygen-dependent
373 enzymes. Our results show that this effect only appears after a first period of hypoxia. It suggests that
374 HIF accumulation forces the cell to adopt a glycolytic state and prevent it from returning to an oxidative
375 state in normoxia. HIF inhibition therapy would prevent the appearance of Warburg cell type in cancer.
376 PI3K and mTOR, two genes that increase HIF level independently of the level of oxygen [11, 14, 13], are
377 studied as potential targets in anti-cancer therapy due to their altered expression in cancer and their role

378 in signalling pathways affecting many biological functions [32, 33], possibly causing HIF overexpression.
379 AMPK enzyme is known to interact with HIF [25] and inhibits its expression, some evidence link this
380 gene to anti-tumour activity [34]. Those interactions could be added in further modelling work to study
381 their impact on the Warburg effect as they may be important players interacting with HIF.

382 It has been shown that extracellular pH can (1) influence the cell metabolism (reduce glucose con-
383 sumption, increase the cells doubling time) [31], (2) affect the ability of tumour cells to form metastasis,
384 invade other tissue or migrate [35] and (3) could be a mechanism of invasion [36]. Currently, therapy
385 targeting extracellular pH in the tumour are under development. Moreover, pH also affects the efficiency
386 of different drugs such as temozolomide [37]. Reducing the increase in LDH level by the cell response
387 to hypoxia lowered the rate of acid production in our simulation. Inhibitor of LDH could be used in
388 combination with pH targeting therapy to improve treatment outcomes.

389 Reducing the down-regulation of PDH by HIF in the model forces the cell to rely as much as possible
390 on oxygen to produce its energy. Herein, changes in metabolism toward glycolytic activity requires lower
391 levels of oxygen. A study has shown that inhibition of HIF resulted in reduced lactate production, increase
392 in oxygen consumption and radiotherapy sensitivity [7]. Whether increasing oxygen consumption by PDH
393 upregulation would result in better outcomes in therapy in the model remains to be studied.

394 Conclusion

395 The main interest of the model is its ability to qualitatively describe HIF expression in tumour devel-
396 opment over time with oxygen diffusion that depends on both cell consumption and cell density in the
397 tumour to obtain a more realistic diffusion. Results of the model show that varying oxygen levels and
398 reduced HIF degradation can cause increased glycolytic activity in normal oxygen levels. In the model,
399 the emergence of the Warburg effect is preceded by a first period of hypoxia before returning to normoxic
400 concentrations. This suggests that adaptation to environmental conditions is the primary phenomenon
401 to understanding the Warburg effect. Interfering with the genetic activity of HIF or its effect on LDH
402 and PDH may be used in therapy to induce specific behaviour in the cell.

403 Acknowledgements

404 We thank Alaa Tafech for providing the picture of the spheroid in Figure 5. This project has received
405 financial support from CNRS through the MITI interdisciplinary programs.

406 Kévin SPINICCI gratefully acknowledges the support of Swansea University Strategic partnership Re-
407 search Scholarship and the support of IDEX Université Grenoble Alpes.

408 Conflicts of Interest

409 The authors declare no conflict of interest.

References

- [1] R. A. Bender. “Glycolysis”. In: *Brenner’s Encyclopedia of Genetics: Second Edition 2* (2013), pp. 346–349. DOI: [10.1016/B978-0-12-374984-0.00659-8](https://doi.org/10.1016/B978-0-12-374984-0.00659-8).
- [2] Thomas C. King. “Cell Injury, Cellular Responses to Injury, and Cell Death”. In: *Elsevier’s Integrated Pathology* (2007), pp. 1–20. DOI: [10.1016/b978-0-323-04328-1.50007-3](https://doi.org/10.1016/b978-0-323-04328-1.50007-3).
- [3] F K Zimmermann. “Glycolysis in *Saccharomyces cerevisiae*”. In: *Encyclopedia of Genetics* (2001), pp. 885–888. DOI: [10.1006/rwgn.2001.0570](https://doi.org/10.1006/rwgn.2001.0570).
- [4] Blanco, Antonio and Gustavo Blanco. “Medical Biochemistry . Academic Press, 2018.” In: (2017), pp. 283–323. DOI: [10.1016/B978-0-12-803550-4/00014-8](https://doi.org/10.1016/B978-0-12-803550-4/00014-8).
- [5] Otto Warburg, Franz Wind, and Erwin Negelein. “The metabolism of tumors in the body”. In: *Journal of General Physiology* 8.6 (1927), pp. 519–530. ISSN: 15407748. DOI: [10.1085/jgp.8.6.519](https://doi.org/10.1085/jgp.8.6.519). URL: <https://www.ncbi.nlm.nih.gov/pmc/articles/PMC2140820/>.
- [6] Pierre Jacquet and Angélique Stéphanou. “Metabolic Reprogramming, Questioning, and Implications for Cancer”. In: *Biology 2021, Vol. 10, Page 129* 10.2 (Feb. 2021), p. 129. ISSN: 20797737. DOI: [10.3390/BIOLOGY10020129](https://doi.org/10.3390/BIOLOGY10020129). URL: <https://www.mdpi.com/2079-7737/10/2/129/html>
<https://www.mdpi.com/2079-7737/10/2/129>.
- [7] Eric Leung et al. “Metabolic targeting of HIF-dependent glycolysis reduces lactate, increases oxygen consumption and enhances response to high-dose single-fraction radiotherapy in hypoxic solid tumors”. In: *BMC Cancer* 17.1 (Dec. 2017), p. 418. ISSN: 1471-2407. DOI: [10.1186/s12885-017-3402-6](https://doi.org/10.1186/s12885-017-3402-6). URL: <https://bmccancer.biomedcentral.com/articles/10.1186/s12885-017-3402-6>.
- [8] Ian F. Robey et al. “Hypoxia-inducible factor-1 α and the glycolytic phenotype in tumors”. In: *Neoplasia* 7.4 (2005), pp. 324–330. ISSN: 15228002. DOI: [10.1593/neo.04430](https://doi.org/10.1593/neo.04430). URL: [/pmc/articles/PMC1501147/?report=abstract](https://www.ncbi.nlm.nih.gov/pmc/articles/PMC1501147/?report=abstract)
<https://www.ncbi.nlm.nih.gov/pmc/articles/PMC1501147/>.
- [9] Mehdi Damaghi et al. “The Harsh Microenvironment in Early Breast Cancer Selects for a Warburg Phenotype”. In: *bioRxiv* (Apr. 2020), p. 2020.04.07.029975. DOI: [10.1101/2020.04.07.029975](https://doi.org/10.1101/2020.04.07.029975). URL: <https://doi.org/10.1101/2020.04.07.029975>.
- [10] S. R. McKeown. *Defining normoxia, physoxia and hypoxia in tumours - Implications for treatment response*. Mar. 2014. DOI: [10.1259/bjr.20130676](https://doi.org/10.1259/bjr.20130676). URL: [/pmc/articles/PMC4064601/](https://www.ncbi.nlm.nih.gov/pmc/articles/PMC4064601/)
[/pmc/articles/PMC4064601/?report=abstract](https://www.ncbi.nlm.nih.gov/pmc/articles/PMC4064601/?report=abstract)
<https://www.ncbi.nlm.nih.gov/pmc/articles/PMC4064601/>.
- [11] Georgina N. Masoud and Wei Li. “HIF-1 α pathway: Role, regulation and intervention for cancer therapy”. In: *Acta Pharmaceutica Sinica B* 5.5 (2015). ISSN: 22113843. DOI: [10.1016/j.apsb.2015.05.007](https://doi.org/10.1016/j.apsb.2015.05.007). URL: <https://www.sciencedirect.com/science/article/pii/S2211383515000817?pes=vor>.

- 445 [12] J. Xu et al. “Epigenetic regulation of HIF-1 α in renal cancer cells involves HIF-1 α /2 α binding to a
446 reverse hypoxia-response element”. In: *Oncogene* 31.8 (2012). ISSN: 09509232. DOI: [10.1038/ncr.](https://doi.org/10.1038/ncr.2011.305)
447 [2011.305](https://pubmed.ncbi.nlm.nih.gov/21841824/). URL: <https://pubmed.ncbi.nlm.nih.gov/21841824/>
448 <https://www.nature.com/articles/ncr2011305>.
- 449 [13] Ji-Won Lee et al. “Hypoxia-inducible factor (HIF -1)alpha : its protein stability and biological
450 function s”. In: *Experimental and Molecular Medicine* 36.1 (2004), pp. 1–12. DOI: [10.1038/emmm.](https://doi.org/10.1038/emmm.2004.1)
451 [2004.1](https://www.nature.com/articles/emmm20041). URL: <https://www.nature.com/articles/emmm20041>.
- 452 [14] Yoshihiro Hayashi et al. “Hypoxia/pseudohypoxia-mediated activation of hypoxia-inducible factor-
453 1 α in cancer”. In: *Cancer Science* 110.5 (May 2019), pp. 1510–1517. ISSN: 1347-9032. DOI: [10.1111/](https://doi.org/10.1111/cas.13990)
454 [cas.13990](https://onlinelibrary.wiley.com/doi/abs/10.1111/cas.13990). URL: <https://onlinelibrary.wiley.com/doi/abs/10.1111/cas.13990>.
- 455 [15] Roger McLendon et al. “Comprehensive genomic characterization defines human glioblastoma genes
456 and core pathways”. In: *Nature* 455.7216 (2008), pp. 1061–1068. ISSN: 00280836. DOI: [10.1038/](https://doi.org/10.1038/nature07385)
457 [nature07385](https://www.nature.com/articles/nature07385). URL: <https://www.nature.com/articles/nature07385>.
- 458 [16] Lucija Slemc and Tanja Kunej. “Transcription factor HIF1A: downstream targets, associated path-
459 ways, polymorphic hypoxia response element (HRE) sites, and initiative for standardization of
460 reporting in scientific literature”. In: *Tumor Biology* 37.11 (2016). ISSN: 14230380. DOI: [10.1007/](https://doi.org/10.1007/s13277-016-5331-4)
461 [s13277-016-5331-](https://link.springer.com/article/10.1007/s13277-016-5331-4)
462 [4](https://link.springer.com/article/10.1007/s13277-016-5331-4).
- 463 [17] Nobuhito Goda, Sara J. Dozier, and Randall S. Johnson. *HIF-1 in cell cycle regulation, apoptosis,*
464 *and tumor progression*. July 2003. DOI: [10.1089/152308603768295212](https://doi.org/10.1089/152308603768295212). URL: [https://www.](https://www.liebertpub.com/doi/abs/10.1089/152308603768295212)
465 [liebertpub.com/doi/abs/10.1089/152308603768295212](https://www.liebertpub.com/doi/abs/10.1089/152308603768295212).
- 466 [18] B. Bedessem and A. Stéphanou. “A mathematical model of HiF-1 α -mediated response to hypoxia
467 on the G1/S transition”. In: *Mathematical Biosciences* 248.1 (2014), pp. 31–39. ISSN: 00255564.
468 DOI: [10.1016/j.mbs.2013.11.007](https://doi.org/10.1016/j.mbs.2013.11.007). URL: <http://dx.doi.org/10.1016/j.mbs.2013.11.007>.
- 469 [19] Jerry J. Zimmerman, Amélie von Saint André-von Arnim, and Jerry McLaughlin. *Cellular Respi-*
470 *ration*. Fourth Edi. Elsevier, 2011, pp. 1058–1072. ISBN: 9780323073073. DOI: [10.1016/B978-0-](https://doi.org/10.1016/B978-0-323-07307-3.10074-6)
471 [323-07307-3.10074-6](http://dx.doi.org/10.1016/B978-0-323-07307-3.10074-6). URL: <http://dx.doi.org/10.1016/B978-0-323-07307-3.10074-6>.
- 472 [20] Wenbo Li and Jin Wang. “Uncovering the Underlying Mechanisms of Cancer Metabolism through
473 the Landscapes and Probability Flux Quantifications”. In: *iScience* 23.4 (Apr. 2020), p. 101002.
474 ISSN: 25890042. DOI: [10.1016/j.isci.2020.101002](https://doi.org/10.1016/j.isci.2020.101002). URL: [https://doi.org/10.1016/j.isci.](https://doi.org/10.1016/j.isci.2020.101002)
475 [2020.101002](https://doi.org/10.1016/j.isci.2020.101002).
- 476 [21] Alvaro Marin-Hernandez et al. “HIF-1alpha Modulates Energy Metabolism in Cancer Cells by
477 Inducing Over-Expression of Specific Glycolytic Isoforms”. In: *Mini-Reviews in Medicinal Chemistry*
478 9.9 (Aug. 2009), pp. 1084–1101. ISSN: 13895575. DOI: [10.2174/138955709788922610](https://doi.org/10.2174/138955709788922610). URL: [http:](http://www.eurekaselect.com/openurl/content.php?genre=article&issn=1389-5575&volume=9&issue=9&spage=1084)
479 [//www.eurekaselect.com/openurl/content.php?genre=article&issn=1389-5575&volume=9&](http://www.eurekaselect.com/openurl/content.php?genre=article&issn=1389-5575&volume=9&issue=9&spage=1084)
480 [issue=9&spage=1084](http://www.eurekaselect.com/openurl/content.php?genre=article&issn=1389-5575&volume=9&issue=9&spage=1084).

- 481 [22] C. Granchi et al. “Inhibitors of Lactate Dehydrogenase Isoforms and their Therapeutic Poten-
482 tials”. In: *Current Medicinal Chemistry* 17.7 (2010), pp. 672–697. ISSN: 09298673. DOI: [10.2174/
483 092986710790416263](https://doi.org/10.2174/092986710790416263). URL: <https://pubmed.ncbi.nlm.nih.gov/20088761/>.
- 484 [23] Shabnam Heydarzadeh et al. *Regulators of glucose uptake in thyroid cancer cell lines*. June 2020.
485 DOI: [10.1186/s12964-020-00586-x](https://doi.org/10.1186/s12964-020-00586-x). URL: <https://doi.org/10.1186/s12964-020-00586-x>.
- 486 [24] Kieran Smallbone et al. “Metabolic changes during carcinogenesis: potential impact on invasive-
487 ness”. In: *Journal of theoretical biology* 244.4 (Feb. 2007), pp. 703–713. ISSN: 0022-5193. DOI:
488 [10.1016/J.JTBI.2006.09.010](https://doi.org/10.1016/J.JTBI.2006.09.010). URL: <https://pubmed.ncbi.nlm.nih.gov/17055536/>.
- 489 [25] Dongya Jia et al. “Elucidating cancer metabolic plasticity by coupling gene regulation with metabolic
490 pathways”. In: *Proceedings of the National Academy of Sciences of the United States of America*
491 116.9 (Feb. 2019), pp. 3909–3918. ISSN: 10916490. DOI: [10.1073/pnas.1816391116](https://doi.org/10.1073/pnas.1816391116). URL: <https://pubmed.ncbi.nlm.nih.gov/30733294/>.
- 493 [26] Rupert Courtney et al. “Cancer metabolism and the Warburg effect: the role of HIF-1 and PI3K”.
494 In: *Molecular biology reports* 42.4 (2015), pp. 841–851. ISSN: 15734978. DOI: [10.1007/s11033-015-
495 3858-x](https://doi.org/10.1007/s11033-015-3858-x).
- 496 [27] Mark Robertson-Tessi et al. “Impact of Metabolic Heterogeneity on Tumor Growth, Invasion, and
497 Treatment Outcomes”. In: *Cancer Research* 75.8 (Apr. 2015), pp. 1567–1579. ISSN: 0008-5472. DOI:
498 [10.1158/0008-5472.CAN-14-1428](https://doi.org/10.1158/0008-5472.CAN-14-1428). URL: [http://cancerres.aacrjournals.org/lookup/doi/
499 10.1158/0008-5472.CAN-14-1428](http://cancerres.aacrjournals.org/lookup/doi/10.1158/0008-5472.CAN-14-1428).
- 500 [28] Ahmadreza Ghaffarizadeh et al. “PhysiCell: An open source physics-based cell simulator for 3-D
501 multicellular systems”. In: *PLOS Computational Biology* 14.2 (Feb. 2018), e1005991. ISSN: 1553-
502 7358. DOI: [10.1371/JOURNAL.PCBI.1005991](https://doi.org/10.1371/JOURNAL.PCBI.1005991). URL: [https://journals.plos.org/ploscompbiol/
503 article?id=10.1371/journal.pcbi.1005991](https://journals.plos.org/ploscompbiol/article?id=10.1371/journal.pcbi.1005991).
- 504 [29] Geoffrey M Cooper. “The Eukaryotic Cell Cycle”. In: (2000). URL: [https://www.ncbi.nlm.nih.
505 gov/books/NBK9876/](https://www.ncbi.nlm.nih.gov/books/NBK9876/).
- 506 [30] Tomás Alarcón and Henrik Jeldtoft Jensen. “Quiescence: A mechanism for escaping the effects of
507 drug on cell populations”. In: *Journal of the Royal Society Interface* 8.54 (2011), pp. 99–106. ISSN:
508 17425662. DOI: [10.1098/rsif.2010.0130](https://doi.org/10.1098/rsif.2010.0130). arXiv: [1002.4579](https://arxiv.org/abs/1002.4579).
- 509 [31] Joseph J. Casciari, Stratis V. Sotirchos, and Robert M. Sutherland. “Variations in tumor cell growth
510 rates and metabolism with oxygen concentration, glucose concentration, and extracellular pH”. In:
511 *Journal of Cellular Physiology* 151.2 (1992), pp. 386–394. ISSN: 10974652. DOI: [10.1002/jcp.
512 1041510220](https://doi.org/10.1002/jcp.1041510220).
- 513 [32] Jing Yang et al. *Targeting PI3K in cancer: Mechanisms and advances in clinical trials*. 2019. DOI:
514 [10.1186/s12943-019-0954-x](https://doi.org/10.1186/s12943-019-0954-x).
- 515 [33] Tian Tian, Xiaoyi Li, and Jinhua Zhang. *mTOR signaling in cancer and mtor inhibitors in solid
516 tumor targeting therapy*. 2019. DOI: [10.3390/ijms20030755](https://doi.org/10.3390/ijms20030755).

- 517 [34] Weidong Li et al. *Targeting AMPK for cancer prevention and treatment*. 2015. DOI: [10.18632/
518 oncotarget.3629](https://doi.org/10.18632/oncotarget.3629).
- 519 [35] S. D. Webb, J. A. Sherratt, and R. G. Fish. “Mathematical Modelling of Tumor Acidity: Regulation
520 of Intracellular pH”. In: *Journal of Theoretical Biology* 196.2 (Jan. 1999), pp. 237–250. ISSN: 0022-
521 5193. DOI: [10.1006/JTBI.1998.0836](https://doi.org/10.1006/JTBI.1998.0836). URL: <https://doi.org/10.1006/jtbi.1998.0836>.
- 522 [36] Kieran Smallbone, Robert A. Gatenby, and Philip K. Maini. “Mathematical modelling of tumour
523 acidity”. In: *Journal of Theoretical Biology* 255.1 (2008), pp. 106–112. ISSN: 00225193. DOI: [10.
524 1016/j.jtbi.2008.08.002](https://doi.org/10.1016/j.jtbi.2008.08.002).
- 525 [37] Angélique Stéphanou and Annabelle Ballesta. “pH as a potential therapeutic target to improve
526 temozolomide antitumor efficacy : A mechanistic modeling study”. In: *Pharmacology Research and
527 Perspectives* 7.1 (Feb. 2019). ISSN: 20521707. DOI: [10.1002/PRP2.454](https://doi.org/10.1002/PRP2.454).